Short-range magnetic order in the paramagnetic phase of cubic $SrMnO_{3-x}$ ($x < 0.005$): An ^{17}O and ^{87}Sr NMR study

A. Gerashenko,[1,2] A. Trokiner,[2] S. Verkhovskii,[1,2] Z. Volkova,[1] A. Germov,[1] K. Mikhalev,[1] and A. Yakubovskii[3]

[1]*Mikheev Institute of Metal Physics, Ural Branch of Russian Academy of Sciences, 620108 Ekaterinburg, Russia*

[2]*LPEM UMR8213, ESPCI Paris, PSL Research University, CNRS, Sorbonne University, 10 rue Vauquelin, Paris, France*

[3]*Russian Research Centre "Kurchatov Institute," 123182 Moscow, Russia*

(Received 29 April 2020; revised 30 July 2020; accepted 15 September 2020; published 8 October 2020)

In the paramagnetic phase of cubic antiferromagnet $SrMnO_{2.997}$ ($T_N = 236$ K), the spin susceptibility of the localized $Mn(t_{2g})$ electrons exhibits a gapped behavior with $d\chi_s(T) \geqslant 0$, suggesting the existence of a low-dimensional short-range magnetic order above T_N. The low-frequency fluctuations of the spin correlations of neighboring Mn^{4+} ions were probed by measuring the spin-lattice relaxation rate T_1^{-1} and the echo-decay rate T_2^{-1} of ^{17}O and ^{87}Sr nuclei up to 420 K. ^{17}O being involved in an Mn–O–Mn bond, the echo-decay rate $^{17}T_2^{-1}$ probes the fluctuations of the two neighboring $S(t_{2g})$ spins at low frequency, $\omega \leqslant 10^3$ s^{-1}. It is shown that there exist local changes of the double-exchange interaction, which favor FM correlated pairs of neighboring $S(t_{2g})$ spins in the Mn–^{17}O–Mn bond. The unusual thermal behavior of $^{17}T_2^{-1}(T)$ indicates low-frequency fluctuations of the short-range magnetic order which may include the change of AF $\leftrightarrow$ FM spin alignment of neighboring magnetic ions. For ^{87}Sr nuclei, which probe the spin configuration of eight neighboring Mn ions in the cubic unit cell, $^{87}T_2^{-1}$ has no such anomaly, implying that FM order should be excluded within *the cubic unit cell*. With both NMR probes, it is deduced that the only magnetic orders which may exist in the *cubic unit cells* are the following: AF–G [$\boldsymbol{q} = \pi/a(1, 1, 1)$], AF–C [$\boldsymbol{q} = \pi/a(1, 1, 0)$], and AF–A [$\boldsymbol{q} = \pi/a(0, 0, 1)$] so that the slow fluctuating short-range magnetic order is built from these three AF ordered unit cells. Furthermore, we deduce from $^{17}T_1^{-1}$ results that the fluctuating short-range magnetic order, i.e., corresponding to large q, has a high thermal stability in the PM phase of $SrMnO_{2.997}$.

DOI: 10.1103/PhysRevB.102.134408

I. INTRODUCTION

The manganese oxides with perovskite structure display a great variety of electronic properties when doped by charge carriers. One of the main issues in the studies of these strongly correlated materials is the ground state emerging from the competition of the antiferromagnetic (AF) superexchange interaction between localized spins and the ferromagnetic (FM) double exchange (DE) interaction of localized spins with itinerant doped carriers.

The lightly electron-doped $SrMnO_{3-x}$ compound appears at first as a simple system with no particular physical properties of great current interest. However, as disclosed in the present research, it is the slight oxygen deficiency that gives rise to unusual dynamic correlations of the localized spins due to the competition of the exchange interactions.

The parent manganese oxide $SrMnO_3$ with the $Pm\bar{3}m$ crystal structure is a rare example of cubic antiferromagnet. Below $T_N \approx 240$ K the magnetic moments of Mn^{4+} ions ($^3t_{2g}{}^0e_g; S = 3/2$) are ordered in two sublattices forming a three-dimensional checkerboard pattern of the G-type AF structure with $\boldsymbol{q}_{AF} = \pi/a(1, 1, 1)$ [1–3]. Cubic $SrMnO_3$ has a high Néel temperature and a small magnetic field anisotropy, $H_a \leqslant 200$ Oe [4]. A similar situation exists in the well known standard cubic AF $RbMnF_3$ ($T_N \approx 83$ K; $H_a \leqslant 5$ Oe [5]). In $RbMnF_3$, the exchange coupling of the Mn^{2+} localized spins ($^3t_{2g}{}^2e_g; S = 5/2$) is well described within the nearest neighbor only Heisenberg model [6,7] showing the classic isotropic AF properties below T_N and the Curie-Weiss behavior in the paramagnetic (PM) phase above $1.3T_N$. Whereas in nominally stoichiometric $SrMnO_3$, the bulk magnetic susceptibility χ increases gradually from T_N reaching a plateau above $1.5T_N$ with no sign of the mean field behavior [2,8–10]. It follows from an ^{17}O NMR study of lightly electron-doped $SrMnO_{3-x}$ ($x < 0.01$) oxides [4] that this gaplike peculiar behavior of the bulk magnetic susceptibility $d\chi/dT \geqslant 0$ should be attributed to the spin susceptibility χ_s of the localized spins of Mn ions, $S(t_{2g})$.

The gaplike T dependence of χ is typical of compounds with low dimensional AF configuration [6]. It implies that for $SrMnO_3$, some short-range magnetic order with a lower-dimensional AF configuration of the $S(t_{2g})$ spins should add to the main three-dimensional AF–G type configuration. In this configuration, each $S(t_{2g})$ spin orders antiferromagnetically with its six nearest neighbors [3]. In contrast to $RbMnF_3$, in $SrMnO_3$, FM correlated pairs of neighboring $S(t_{2g})$ spins may appear due to the $t_{2g} - e_g$ electron hopping at empty doubly degenerate e_g orbital [11]. The broad e_g-orbital degenerate conduction band, $W \sim 2$ eV, allows a gain in kinetic energy for the e_g electrons placing the *undoped* cubic $SrMnO_3$ close to the borderline between the metallic and insulating states.

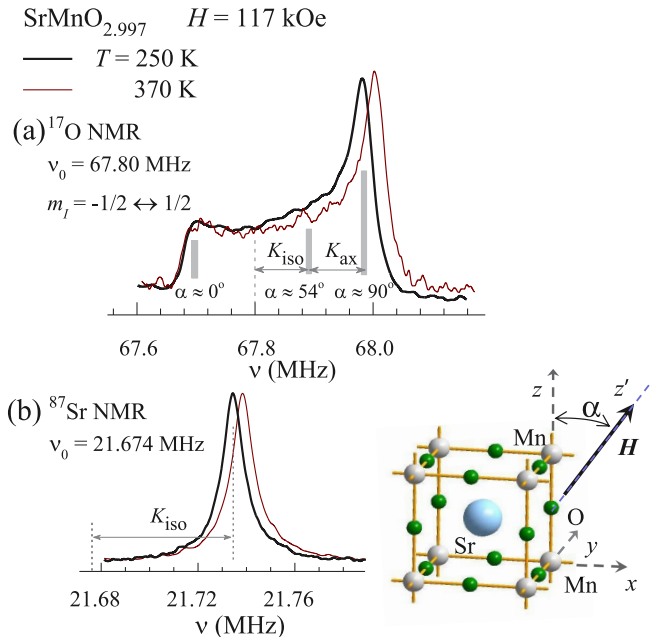

FIG. 1. Paramagnetic phase of polycrystalline cubic $SrMnO_{2.997}$ sample. (a) Central line (transition $m_I = -1/2 \leftrightarrow +1/2$) of ^{17}O NMR spectra and (b) ^{17}Sr NMR spectra including all the transitions. The angle α is determined by the direction of the external magnetic field $\boldsymbol{H}$ relative to the Mn–O–Mn bond direction.

Furthermore, in lightly e-doped $SrMnO_3$ the energy barrier, separating AF phases with different magnetic unit cell characterized by FM correlated planes (A type [3]) or FM correlated chains (C type [3]) of the Mn^{4+} ions is comparable to $k_B T_N \approx 0.03$ eV [12,13] so that short-wavelength AF phase fluctuations may exist. If these fluctuations exist, they should be enhanced along the path of the diffusing motion of the doped e_g electrons [14] by the double-exchange mechanism [15]. To our knowledge, there are no studies of low-energy spin excitations in the PM phase because of the absence of large enough $SrMnO_3$ single crystals for neutron experiments.

Our recent NMR studies have shown the efficiency of ^{17}O [4] and ^{87}Sr [16] NMR probes to investigate the *static* spin correlations of the neighboring Mn^{4+} ions in lightly doped $SrMnO_{3-x}$. Some basic results of these NMR studies are used in the present research focusing on the Mn *dynamic* spin correlations in the PM phase of $SrMnO_{3-x}$ ($x < 0.005$).

In the perovskite structure, an oxygen atom is directly involved in the formation of both covalent chemical bond and anisotropic superexchange interaction between the localized $S(t_{2g})$ spins of neighboring Mn. The transferred spin on the $O(2p_\pi)$ orbital $s(2p_\pi) = f_\pi S_z(t_{2g})$, creates the main contribution, $^{17}K_{ax}(2p_\pi)$, to the anisotropic hyperfine shift of the ^{17}O NMR line: $K_{hf}(\alpha) = K_{ax,hf}(3\cos^2\alpha - 1)$, where α is the angle between $\boldsymbol{H}$, the experimental magnetic field and the straight Mn–O–Mn bond (Fig. 1). At $x \ll 1$ [17],

$$\begin{aligned} {}^{17}K_{ax}(2p_\pi) &= h_{ax}(2p_\pi)/H \\ &= -4/5\mu_B\langle r^{-3}\rangle_{2p} f_\pi(\langle S_{z1}(t_{2g}) + S_{z2}(t_{2g})\rangle)/H \\ &= H(2p_\pi) f_\pi(\langle S_{z1}(t_{2g}) + S_{z2}(t_{2g})\rangle)/H, \end{aligned} \quad (1)$$

where f_π is the fractional occupancy of the $O(2p_\pi)$ orbital by an unpaired Mn spin and the thermal average $\langle S_z(t_{2g})\rangle$ relates to $\chi_s = g\mu_B\langle S_z(t_{2g})\rangle/H$, the local spin susceptibility of Mn^{4+} ion, the nearest neighbor of the ^{17}O probe. A *negative* value $^{17}K_{ax}(2p_\pi) < 0$, following from Eq. (1), defines an asymmetrical shape of the central line (Fig. 1) which intensity is maximum at a higher frequency relative the gravity center, $^{17}K_{iso}$. Whereas the transferred spin on the $O(2p_\pi)$ orbital, which lobes are directed along Mn–O–Mn bond, creates a *positive* shift $^{17}K_{ax}(2p_\sigma) > 0$. This shift is negligible in $SrMnO_{3-x}$ ($x \ll 1$) because of the almost zero occupancy of the $Mn(e_g)$ orbital, $Mn(e_g)$ being the counterpart in $Mn(e_g)$–$O(2p_\sigma)$ covalency (Eqs. (5) and (6) in Ref. [4]). Thus the temperature dependence of $|K_{ax}|$ is the one of $\chi_s(T)$.[1]

The isotropic component of the hyperfine magnetic shift $^{17}K_{iso}$ arises *only in doped* $SrMnO_{3-x}$. It is due to the Fermi contact interaction of the nuclear spin ^{17}I with spin density $s_z(2s) = f_{2s}s_z(e_g) = f_{2s}n_{e_g}J/E_F\langle S_z(t_{2g})\rangle$, created by the n_{e_g} fast-moving doped electrons, with $n_{e_g} \leqslant 2x$. The n_{e_g} electrons become itinerant in the conduction band $O(2s)$–$Mn(e_g)$, having a dominant e_g character [14,18]. Because of the strong intra-atomic exchange interaction with the almost localized t_{2g} electrons, $-J_s(e_g)S(t_{2g})$, the band consists of spin-up polarized states with the density of states $g(E_F) \sim n_{e_g}/E_F$ when $x \ll 1$ [12], and

$$\begin{aligned} {}^{17}K_{iso} &= {}^{17}h(e_g)/H \\ &= H_{FC}(2s) f_{2s}(J_H/E_F) n_{e_g}(\langle S_{z1}(t_{2g})\rangle + \langle S_{z2}(t_{2g})\rangle)/H \\ &= {}^{17}H(e_g) n_{e_g}(\langle S_{z1}(t_{2g})\rangle + \langle S_{z2}(t_{2g})\rangle)/H. \end{aligned} \quad (2)$$

Here, the hyperfine magnetic field, $H_{FC}(2s)$, is created by one unpaired electron residing at the $O(2s)$ orbital. According to Eqs. (1) and (2), the ratio $K_{iso}(T)/|K_{ax}|$ is proportional to $n_{e_g}/2x$, the fraction of the fast-moving doped electrons per Mn. Only these fast-moving n_{e_g} electrons provide the ^{17}O NMR shift,$^{17}K_{iso}$, defined by Eq. (2).

The same reasoning is valid for ^{17}Sr NMR. In $SrMnO_3$ the Sr atom has eight nearest Mn neighbors. The corresponding isotropic hyperfine shift, $^{87}K_{iso}$, is caused by the spin densities $s_z(5s) = f_{5s}s_z(e_g) = f_{5s}n_{e_g}J/E_F\langle S_{z,i}(t_{2g})\rangle$, transferred to the $Sr(5s)$ orbital by each magnetic neighbor:

$$\begin{aligned} {}^{87}K_s &= {}^{87}h(e_g)/H \\ &= H_{FC}(5s) f_{5s}(J/E_F) n_{e_g} \Sigma_i \langle S_{z,i}(t_{2g})\rangle/H \\ &= {}^{87}H(e_g) n_{e_g} \Sigma_i \langle S_{z,i}(t_{2g})\rangle/H. \end{aligned} \quad (3)$$

In addition, it was shown that in the AF ordered phase at low temperature, all doped electrons have slowed down the Mn–Mn hopping. In this situation, there is an increase of FM interaction between Mn neighbors by means of the DE mechanism [19] leading to the formation of small-size magnetic polarons in the G-type AF matrix. These polarons were detected below 10 K by ^{55}Mn NMR [4].

[1]In $SrMnO_3$, the contribution $K_{ax,dip}$ of the classic dipolar fields from neighboring induced Mn^{4+} moments $m_{z||H}(Mn) = \chi_{mol}H/N_A$ is about three time smaller than $|^{17}K_{ax}(2p_\pi)|$ [4]. Thus the value of $^{17}K_{ax}(2p_\pi)$ was obtained in the following way: $^{17}K_{ax}(2p_\pi) = K_{ax,measured} - K_{ax,dip}$.

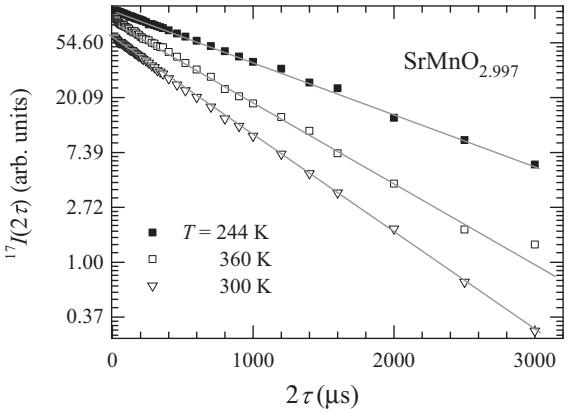

FIG. 2. Integral of the spectral intensity $^{17}I(2\tau)$ of the ^{17}O NMR central line at $\alpha \approx 54^\circ$ as a function of 2τ (see text). The solid lines are the fit with a single exponential decay $^{17}I_\alpha(2\tau) \propto \exp(-2\tau/\,^{17}T_2)$.

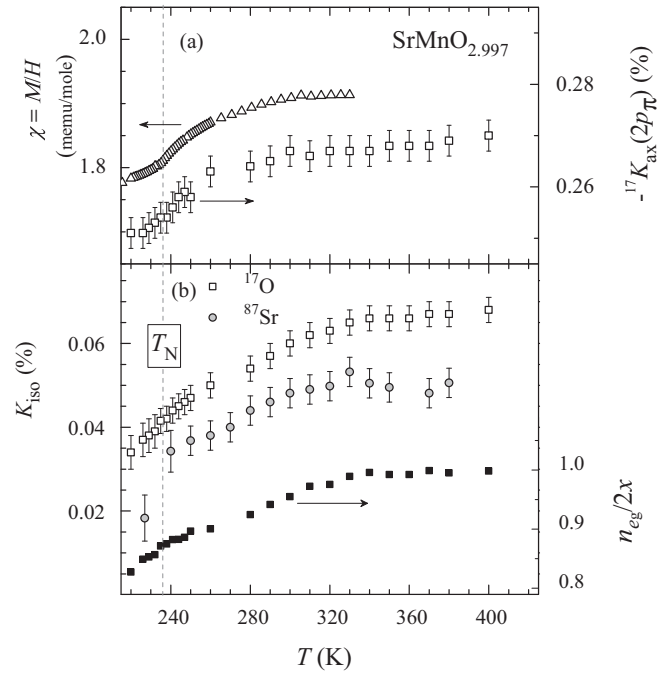

FIG. 3. Temperature dependence of (a) the bulk magnetic susceptibility $\chi = M/H$; the axial hyperfine component $^{17}K_{ax}(2p_\pi)$ of the ^{17}O NMR shift, and (b) isotropic hyperfine NMR shift K_{iso} of both nuclei ^{17}O and ^{17}Sr; $n_{e_g}/2x$ is the fraction per Mn atom of the fast-moving doped electrons.

In this paper, we study the time-dependent part of the hyperfine fields $^{17}h(e_g)$, $^{87}h(e_g)$, and $^{17}h(2p_\pi)$ at low frequencies by measuring the spin-lattice relaxation rate T_1^{-1} and the spin-echo decay rate T_2^{-1} of ^{17}O and ^{17}Sr nuclei. The results shed light on the slow-fluctuating short-range correlations between the localized Mn spins, $S(t_{2g})$, in the PM phase of a lightly electron doped cubic $SrMnO_{3-x}$ polycrystalline sample, i.e., $SrMnO_{2.997}$ ($x < 0.005$). A description of the short-range magnetic orders is inferred.

II. EXPERIMENTAL DETAILS

The $SrMnO_{2.997}$ polycrystalline sample with the cubic structure was synthesized following the procedure described in Ref. [4]. At the last stage of synthesis the sample was annealed during 24 hours at $T = 500\,^\circ$C in oxygen flow ($P_{O2} =$ 1 bar) containing 70% of ^{17}O isotope, for ^{17}O NMR measurements. According to x-ray diffraction the ^{17}O-enriched sample has the $Pm\bar{3}m$ perovskite structure with the unit cell parameter $a = 3.8062(4)$ Å at room temperature. In order to estimate the oxygen content of our sample, $3 - x = 2.997$, we used a phenomenological dependence law of the lattice cell parameter versus the oxygen deficiency, $a(x)$, which was suggested in Ref. [4] for cubic $SrMnO_{3-x}$ compounds with $x < 0.01$. Let us note that a slightly less doped ^{17}O-enriched sample, $SrMnO_{2.998}$, was described in Ref. [4]. We use their $^{17}T_2$ data at room temperature in Sec. III C.

Magnetization measurements were carried out with a magnetometer PPMS-9 (Quantum Design) on cooling the sample in magnetic field $H = 90$ kOe. The corresponding dc magnetic susceptibility $\chi = M/H$ demonstrates a plateaulike behavior in a broad temperature range above $T_N =$ 236(2) K with no signature of the Curie-Weiss law dependence [Fig. 3(a)].

The ^{17}O and ^{17}Sr NMR measurements were performed with AVANCE II(III) – 500WB (Bruker) NMR spectrometer in the temperature range $200 - 400$ K and $H = 117$ kOe. The broad NMR spectra of both, ^{17}O (spin $^{17}I = 5/2$) and ^{17}Sr ($^{87}I = 9/2$) nuclei (Fig. 1) were obtained by summing the Fourier-transformed half-echo signals acquired at equidistant (80 KHz) operating frequencies. The ^{17}O (^{17}Sr) NMR shifts $^{17(87)}K$ are defined relative to the Larmor frequency $^{17}\nu_0 = 67.80$ MHz ($^{87}\nu_0 = 21.67$ MHz), $^{17(87)}K = (\nu - {}^{17(87)}\nu_0)/\,{}^{17(87)}\nu_0$.

The spin-lattice relaxation rate of ^{17}O nuclei $^{17}T_1^{-1}$ was measured on the central line of the ^{17}O NMR spectrum (Fig. 1) by the inversion-recovery technique using the pulse sequence $2p$-t_{inv}-p-τ-p-τ-echo signal $^{17}E(t_{inv})$ with fixed delay $\tau =$ 30 μs, variable $t_{inv} = 0.01$–250 ms and a pulse duration $p =$ 1.6 μs. At each t_{inv}, the integral of spectral intensity of the line $I_\alpha(t_{inv})$ taken in the frequency range $\nu_\alpha \pm 0.005$ MHz was measured, where ν_α corresponds to the angle α. At $\alpha_{magic} = \arccos(1/\sqrt{3}) = 54.7^\circ$, all nuclear m_I levels of ^{17}O are equidistant so that the $\{I_\alpha(t_{inv})\}$ data array is well described by a single-exponential dependence [20]: $(I_{\alpha,0} - I_\alpha(t_{inv})) \propto \exp(-t_{inv}/\,^{17}T_1)$, where $I_{\alpha,0} = I_\alpha(t_{inv})$ at $t_{inv} \geqslant 5T_1$. The rate $^{17}T_1^{-1}$ was determined also at $\alpha = 40^\circ$ and 70° aiming to evaluate the anisotropic contribution $^{17}T_1^{-1}(2p_\pi) \propto (2 + 3\sin^2\alpha)$ of the fluctuating hyperfine field $h_{ax}(2p_\pi)$. The value of $^{17}T_1$ was approximated by a single-exponential fit of $\{I_\alpha(t_{inv})\}$ raw data in the range $0.5T_1 \leqslant t_{inv} \leqslant 5T_1$.

For ^{17}Sr nuclei, the spin-lattice relaxation rate $^{87}T_1^{-1}$ was measured at the peak of the spectrum (Fig. 1) using the pulse sequence p-τ-p-τ-echo signal $^{87}E(2\tau, t)$ with fixed $\tau =$ 100 μs, $p = 3$ μs and variable repetition time of the pulse sequence, $t = 0.005$–2 s. Over the entire temperature range the excitation bandwidth [21] $(\delta\nu)_{BW} = 2.8/\pi p = 300$ KHz is three times larger than the width of the ^{17}Sr NMR spectra which includes all $2 \times {}^{87}I = 9$ transitions. Indeed, the NMR spectrum of the quadrupolar nuclei ^{17}Sr ($^{87}Q = 0.15$ barn)

has no quadrupolar splitting due to the cubic symmetry, in average, of the ^{17}Sr electrical environment as shown in Fig. 1. Because of that, the method for measuring $^{87}T_1$ yields a single exponential recovery.

The spin-echo decay rate T_2^{-1} of ^{17}O and ^{17}Sr nuclei were measured using the pulse sequence p-τ-2p-τ-echo signal $E(2\tau)$, with $p(^{17}O) = 1.6$ μs; $p(^{87}Sr) = 3$ μs. For ^{17}Sr nuclei, the measurements were performed at the peak of the ^{17}Sr NMR spectrum. The intensity of the echo signal $I(2\tau)$ was acquired as a function of τ, the delay between the pulses. The $^{87}T_2$ value was determined by fitting of the $\{^{87}I(2\tau)\}$ data array with the expression $^{87}I(2\tau) = I(0)\exp(-2\tau/^{87}T_2)$. For ^{17}O nuclei, the integral of the spectral intensity of the central line $^{17}I_\alpha(2\tau) \propto {}^{17}E_\alpha(2\tau)$ was considered. This integral was measured in the frequency range $\nu_\alpha \pm 0.005$ MHz and as a function of 2τ, at fixed ν_α, where ν_α corresponds to the angle α. Some representative $^{17}I_\alpha(2\tau)$ raw data collected at $\alpha_{\text{magic}} = 54.7^\circ$ and at different temperatures are plotted in a semilogarithmic scale in Fig. 2. As can be seen on the figure the drop of the echo signal $^{17}I_\alpha(2\tau)$ on more than e^3 times is well described by a single exponential dependence over the entire temperature range.

III. RESULTS AND DISCUSSION

A. Static spin susceptibility traced by ^{17}O and ^{87}Sr NMR shift

Figure 1 shows at $T = 250$ and 370 K the central line (transition $m_I = -1/2 \leftrightarrow +1/2$) of the ^{17}O NMR and the ^{17}Sr NMR spectra which include all the $2 \times I = 9$ transitions. For both probe nuclei, the spectra are shifted toward higher frequencies relative to the corresponding Larmor frequency $^{17(87)}\nu_0$ so that the hyperfine isotropic shifts $^{17(87)}K_{\text{iso}}$ are positive; their growth with T is shown in Fig. 3(b).

(1) The growth with temperature of the hyperfine axial shift $|\,^{17}K_{\text{ax}}(2p_\pi)| \propto \chi_s$ confirms the gaplike $d\chi_s/dT \geqslant 0$ behavior of static spin susceptibility of the localized $S(t_{2g})$ spins in the PM phase of $SrMnO_{2.997}$ [Fig. 3(a)].

(2) Below 350 K the ratio $^{17}K_{\text{iso}}(T)/|\,^{17}K_{\text{ax}}(T)|$ decreases. As it is proportional to n_{e_g}, the number of fast-moving doped electrons, the decrease indicates that the number of slow-moving electrons $(2x - n_{e_g})$ grows [Fig. 3(b)]. These doped electrons slow down their rate of Mn–Mn hopping, thus locally enhancing the FM interaction of their Mn neighbors by means of the DE mechanism [19]. With decreasing T the time τ during which such electrons are near Mn ions, increases following the Arrhenius law $\tau(T) \propto \exp(E_a/T)$ where the energy barrier E_a is about 300 K. Below 50 K when $\tau \geqslant 6 \times 10^{-9}$ s, these slow-moving electrons create static FM nanodomains.

(3) In the PM phase, the slow-moving $(2x - n_{e_g})$ electrons create along their diffusion path the local field h_{FM}, which is far larger than the $h(e_g)$ value defined by Eqs. (2) and (3). So that during the time $\tau \ll 2\pi/\omega_0$, the local field h_{FM} shifts the resonance frequency of the $^{17(87)}I$ neighbors out of the NMR window studied in this work and shown in Fig. 1. Consequently, and as it is observed, no static magnetic broadening of the $^{17(87)}$NMR spectra should occur when T decreases. These pulselike fluctuations of the local field, caused by slow-moving $(2x - n_{e_g})$ electrons, may have an impact on the nuclear spin relaxation of both NMR probes as explained below.

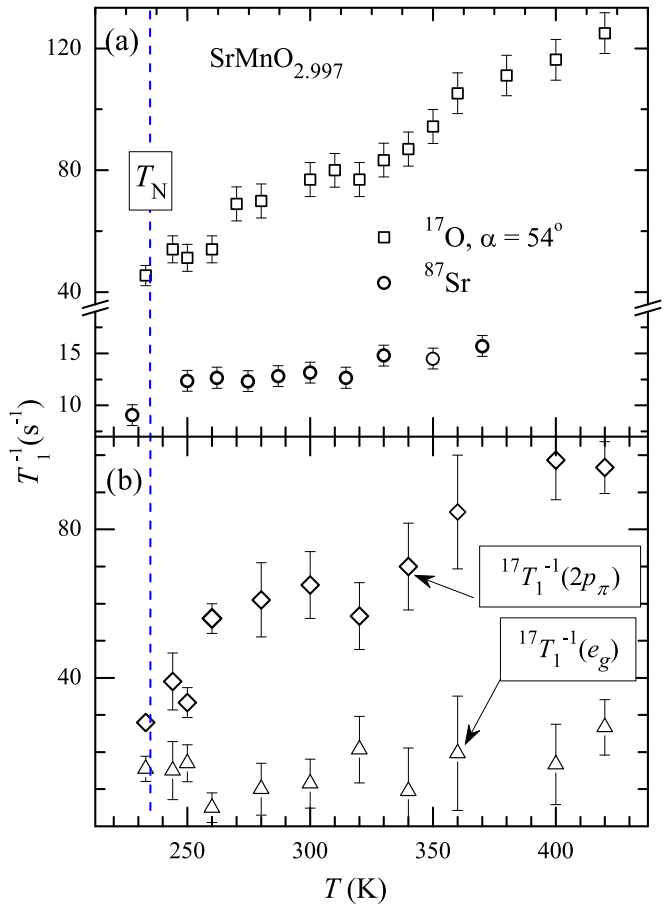

FIG. 4. Temperature dependence of (a) the spin-lattice relaxation rate T_1^{-1} of ^{17}O ($\alpha = 54^\circ$) and ^{17}Sr nuclei, and (b) isotropic $^{17}T_1^{-1}(e_g)$ and anisotropic $^{17}T_1^{-1}(2p_\pi)$ contributions to $^{17}T_1^{-1}$ at $\alpha = 54^\circ$.

B. Spin-lattice relaxation of ^{17}O and ^{17}Sr nuclei

Figure 4(a) shows the thermal behavior of the spin-lattice relaxation rate T_1^{-1} of ^{17}O ($\alpha = 54^\circ$) and ^{17}Sr nuclei. Above T_N, both rates $^{17}T_1^{-1}$ and $^{87}T_1^{-1}$ are roughly proportional to T.

Let us consider $^{17}T_1^{-1}(\alpha, T)$. According to Eqs. (1) and (2), its value is contributed by the time fluctuating part of the isotropic hyperfine field $h(e_g)$, $^{17}T_1^{-1}(e_g)$, and of the α-dependent hyperfine field $h(2p_\pi)$ with $^{17}T_1^{-1}(2p_\pi) \propto (2 + 3\sin^2\alpha)$ [22]:

$$^{17}T_1^{-1}(\alpha) = {}^{17}T_1^{-1}(2p_\pi) + {}^{17}T_1^{-1}(e_g). \quad (4)$$

More precisely, $^{17}T_1^{-1}(2p_\pi)$ is due to the time dependence of the transverse component $h_\perp(2p_\pi)$, which originates from the fluctuations at the frequency $\omega = {}^{17}\gamma H$ of the transverse $S_{i,x'(y')}$ components of the localized $S(t_{2g})$ spins of neighboring Mn^{4+} ions through the corresponding spin transfer $s_{x'(y')}(2p_\pi) = f_\pi S_{x'(y')}(t_{2g})$ on the $O(2p_\pi)$ orbital [23]. The transverse component $h_\perp(2p_\pi)$ of the hyperfine field $h(2p_\pi)$ lies in the $x'y'$ plane orthogonal to $\boldsymbol{H} \parallel \boldsymbol{z}'$ and is defined as $h_\perp(2p_\pi) = H(2p_\pi)f_\pi\{S_{1,x'(y')}(t_{2g}) + S_{2,x'(y')}(t_{2g})\}$. These two

contributions to $^{17}T_1^{-1}(\alpha)$, having different α dependencies, were separated from each other by measuring the rate $^{17}T_1^{-1}$ at $\alpha = 40°$, 54°, and 70°. As seen on Fig. 4, the magnitude and T dependence of $^{17}T_1^{-1}$ are determined by $^{17}T_1^{-1}$ $(2p_\pi)$.

$$^{17}T_1^{-1}(2p_\pi) = \frac{\gamma^2 k_B}{16\mu_B^2}(H(2p_\pi)f_\pi)^2 T(2+3\sin^2\alpha) \times \Sigma_q \cos^2(q_z a/2)\chi_s''(q,\omega)/\omega. \quad (5a)$$

The factor $(2 + 3\sin^2\alpha)$ takes into account the α dependence of $^{17}T_1^{-1}(2p_\pi)$, $\chi_s''(q,\omega) \propto \int_0^\infty d\tau \langle S_q(\tau)S_q(0)\rangle \cos(\omega\tau)$ is the imaginary part of the dynamic spin susceptibility. Its value determines the spectral intensity of the q component of the correlation function of the fluctuating neighboring $S(t_{2g}, t)$ spins at the frequency ω. Because the $^{17}T_1^{-1}$ data were obtained at $\omega_{NMR} \ll \omega_{ex}$ where $\omega_{NMR} = {}^{17}\gamma H = 4 \times 10^8$ s^{-1} and $\omega_{ex} \approx 5.8 \times 10^{12}$ s^{-1} Ref. [13], we may approximate $\chi_s''(q,\omega)/\omega \approx \chi_s'(q)/\omega_{sf}$. Furthermore, the long-wavelength terms with $q \ll \pi/a$ are the only significant terms in the summation of Eq. (5) because of the specific q dependence of the form-factor. After reducing $\Sigma_q \cos^2(q_z a/2)\chi_s''(q,\omega)/\omega \to \Sigma_{q\sim 0}\chi_s'(q)/\omega_{sf}(q) \to \chi_s(q=0)/\omega_{sf}$, Eq. (5) takes the final form:

$$^{17}T_1^{-1}(2p_\pi) = \frac{\gamma^2 k_B}{16\mu_B^2}(H(2p_\pi)f_\pi)^2 \times T(2+3\sin^2\alpha)\chi_s(q=0)/\omega_{sf}, \quad (5b)$$

where $\chi_s(q=0)$ is the uniform $(q=0)$ spin susceptibility of the localized $S(t_{2g})$ spins. The almost T-independent behavior of $\chi_s(q=0)$ is well traced by static ^{17}O NMR data.

The linear growth with T of $^{17}T_1^{-1}(2p_\pi)$ indicates an almost T-independent value of $\hbar\omega_{sf}$, the characteristic energy of the damped magnon excitations, at $q \ll \pi/a$ of AF coupled $S(t_{2g})$ spins in the PM phase of $SrMnO_{2.997}$ with $\hbar\omega_{sf} = 2.5(7)$ meV.[2] This value is about 1.5 times less than the exchange energy $\hbar\omega_{ex}(q=\pi/a) = 3.8(2)$ meV, i.e., $5.8(1) \times 10^{12}$ s^{-1}, estimated at $T_N = 236$ K. In a classic AF scenario, just above T_N a peak of $\chi_s(q)$ at $q \sim \pi/a$ is expected; as T increases in the PM phase, this peak is more or less smeared out so that $\chi_s(q)$ at $q \sim q_{AF}$ decreases while $\chi_s(q)$ at $q \sim 0$ increases. That is why the T-independent behavior of the $\chi_s(q)/\omega_{sf}(q)$ ratio at $q \sim 0$ is unexpected; it could imply that even far above T_N some peak of $\chi_s(q)$ at $q \sim q_{AF}$ would still exist. Thus the $^{17}T_1^{-1}$ results indirectly indicate a high thermal stability of the fluctuating short-range magnetic order (SRMO) in the PM phase of $SrMnO_{2.997}$, unlike $RbMnO_3$, where a thermally fragile SRMO was observed only up to $1.1T_N$ in inelastic neutron scattering experiments [24].

As seen in Fig. 4, the increase with T of $^{17}T_1^{-1}(e_g)$ and $^{87}T_1^{-1}$ is less pronounced than for $^{17}T_1^{-1}(2p_\pi)$. According to Eqs. (2) and (3) their values are defined by the spectral intensity, built at $^{17(87)}\omega_{NMR}$ by the product of two correlation functions: $\langle n_{e_g}(t)n_{e_g}(0)\rangle$ relevant to the fast moving doped e_g electrons and $\langle S_q(t)S_q(0)\rangle$ of the localized $S(t_{2g})$ spins. The small variation of $^{17}T_1^{-1}(e_g)$ and $^{87}T_1^{-1}$ (Fig. 4) shows that, in the frequency range $^{17(87)}\omega_{NMR} = (1\text{–}4) \times 10^8$ s^{-1}, the spectral intensity is not much influenced by $\langle n_{e_g}(t)n_{e_g}(0)\rangle$. In contrast, at very low frequencies $\langle n_{e_g}(t)n_{e_g}(0)\rangle$ leads to an abnormal growth of the fluctuating $^{17}h(e_g)$, as seen below.

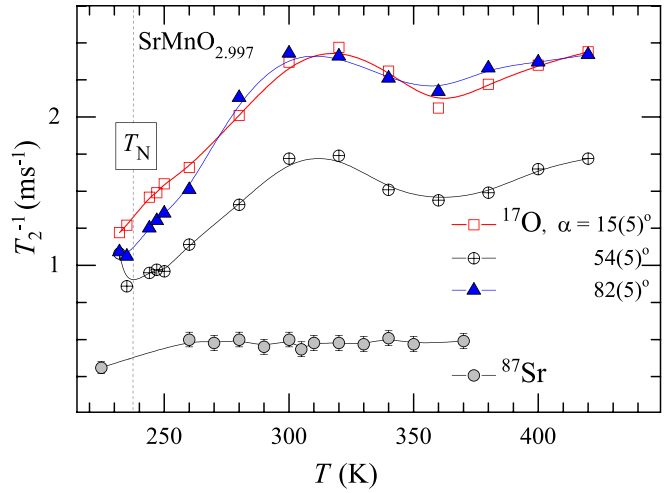

FIG. 5. Thermal behavior of ^{17}O and ^{87}Sr spin-echo decay rates in $SrMnO_{2.997}$. The angle α defines the direction of the magnetic field $\boldsymbol{H}$ relative to the Mn–O–Mn bond direction.The solid curves are guide for the eye.

C. ^{17}O and ^{87}Sr spin-echo decay rate

The thermal behavior of the spin-echo decay rates are shown on Fig. 5. Unlike the almost constant value of $^{87}T_2^{-1}$, the $^{17}T_2^{-1}$ rate increases with T passing through a broad peak around $T = 310$ K, whatever the value of the angle α.

Compared to $^{17(87)}T_1^{-1}$ which is only proportional to $h_\perp^2$, the spin-echo decay rate is determined by both time-dependent components: $h_\perp \perp \boldsymbol{H}$ at $\omega = {}^{17(87)}\omega_{NMR}$ and $h_\parallel \parallel \boldsymbol{H}$ at much lower frequency, $\omega \leqslant 10^3$ s^{-1}, of the corresponding hyperfine fields $^{17}h(2p_\pi)$, $^{17}h(e_g)$, and $^{87}h(e_g)$ [23]:

$$^{17(87)}T_2^{-1} = {}^{17(87)}T_2^{-1}(h_\parallel) + {}^{17(87)}(T_{1,\text{echo}}(h_\perp))^{-1}. \quad (6)$$

The contribution $(T_{1,\text{echo}})^{-1}$ in Eq. (6) is enhanced compared to the corresponding spin-lattice relaxation rate T_1^{-1}. As Eqs. (6a) and (6b) show, the enhancement depends on the fluctuating local field. For ^{17}Sr nuclei, it is

$$^{87}(T_{1,\text{echo}})^{-1} = \left({}^{87}I + 1/2\right)^2 ({}^{87}T_1(e_g))^{-1}. \quad (6a)$$

For ^{17}O nuclei, the second term in Eq. (6) depends on α [25,26]. Compared with previous $^{17}T_2^{-1}$ consideration presented in Ref. [4] at room temperature for the less doped $SrMnO_{2.998}$, we use here an expression for the $^{17}T_{1,\text{echo}}(h_\perp)^{-1}$ rate taking into account both an isotropic contribution of doped electrons, $^{87}T_1(e_g)^{-1}$, and anisotropic contribution of localized $S(t_{2g})$ spins, $^{17}T_1^{-1}(2p_\pi)$:

$$(^{17}T_{1,\text{echo}})^{-1} = (^{17}I + 1/2)^2(^{17}T_1(e_g))^{-1} + (5.25 + 5.625\sin^2\alpha)(^{17}T_1(2p_\pi, \alpha = 54°)^{-1}), \quad (6b)$$

[2]The ω_{sf} $(q \ll \pi/a)$ value was estimated using Eq. (5a) with the $^{17}T_1^{-1}(2p_\pi)$ rate in Fig. 4(b) and the product $H(2p_\pi)f_\pi = 7$ kOe deduced from Eq. (1) and the $^{17}K_{ax}$ and $\chi = M/H$ data in Fig. 3.

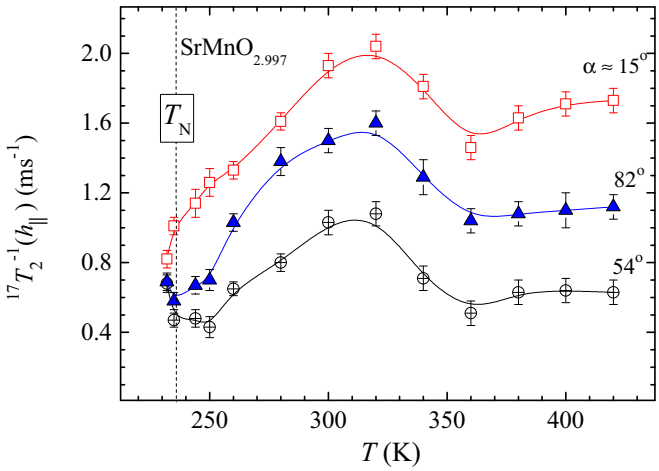

FIG. 6. Temperature dependence of $^{17}T_2^{-1}(h_\parallel)$ for different values of the angle α.

where the $(^{17}T_1(e_g))^{-1}$ and $^{17}T_1{}^{-1}(2p_\pi, \alpha = 54^\circ)$ values are shown at each temperature in Fig. 4. For both nuclei, $(T_{1,\text{echo}})^{-1}$ varies monotonically with temperature. By subtracting these terms from the measured data $(T_2^{-1})_{\text{exp}}$, the spin-echo decay rate $T_2^{-1}(h_\parallel)$ defined by the fluctuations of $h_\parallel$ is obtained:

$$^{17}T_2^{-1}(h_\parallel) = \left(T_2^{-1}\right)_{\text{exp}} - (T_{1,\text{echo}})^{-1} = {}^{17}T_{2,e_g}^{-1}(h_\parallel) + {}^{17}T_{2,2p_\pi}^{-1}(h_\parallel). \quad (7)$$

Figure 6 shows the T dependence of $^{17}T_2^{-1}(h_\parallel)$ for $\alpha = 15^\circ$, 54°, and 82°. The two terms in Eq. (7) are due to the isotropic fluctuations of the hyperfine field $^{17}h(e_g)$ and anisotropic fluctuations of the hyperfine field $^{17}h(2p_\pi) \propto (1 - 3\cos^2\alpha)$, respectively. Let us consider the α dependence of $^{17}T_2^{-1}(h_\parallel)$. Figure 7 shows $^{17}T_2^{-1}(h_\parallel)$ as a function of the angle α for $SrMnO_{2.997}$ ($x = 0.003$) at $T = 244$ and 420 K, and for the less doped $SrMnO_{2.998}$ ($x = 0.002$) [4] at $T = 300$ K. At each temperature the $\{^{17}T_{2,\alpha}^{-1}(h_\parallel)\}$ data array was fitted with the expression $a + b(1 - 3\cos^2\alpha)^2$ aiming to determine both the isotropic $^{17}T_{2,e_g}^{-1}(h_\parallel) \equiv a$ and anisotropic $^{17}T_{2,2p_\pi}^{-1}(h_\parallel) \equiv b(1 - 3\cos^2\alpha)^2$ contributions. Their temperature dependencies are shown in Fig. 8.

Comparing $SrMnO_{2.997}$ to the less doped $SrMnO_{2.998}$ sample, the value of $^{17}T_{2,2p_\pi}^{-1}(h_\parallel)$ is not changed, unlike the contribution $^{17}T_{2,e_g}^{-1}(h_\parallel)$, as seen on Fig. 8(a). As $^{17}T_{2,2p_\pi}^{-1}(h_\parallel)$ shows no dependence on x, it is expected to be the same in the stoichiometric ($x = 0$) $SrMnO_3$, where $^{17}T_{2,2p_\pi}^{-1}(h_\parallel)$ is caused by fast fluctuations ($\omega_{\text{ex}} \gg {}^{17}\omega_0$) of the exchange-coupled localized $S(t_{2g})$ spins. In the scenario of the nearest-neighbor AF exchange interaction, the spins $\boldsymbol{S}_1, \boldsymbol{S}_2$ of the two neighboring Mn1, Mn2 spend all the time in the ground singlet state ($\boldsymbol{S}_1 + \boldsymbol{S}_2 = 0$). The local field $h_\parallel(t)$ created by these spins at oxygen has no vanishing mean square value $\langle(h_{\parallel,\text{singlet}})^2\rangle \sim (^{17}K_{\text{hf,ax}}H)^2$. As for $^{17}\omega_0/\omega_{\text{ex}} \ll 1$, the rate $^{17}T_{2,2p_\pi}^{-1}(h_\parallel)$ can be written as $\gamma^2\langle(h_{\parallel,\text{singlet}})^2\rangle \times 2\pi/\omega_{\text{ex}}$ [23], $^{17}T_2^{-1}(h_\parallel)$ is thus estimated to be 0.5 s^{-1}. This value is far smaller than the experimental rate $^{17}T_2^{-1}(h_\parallel) = 0.2$–$0.3$ ms^{-1} shown on Fig. 8(b).

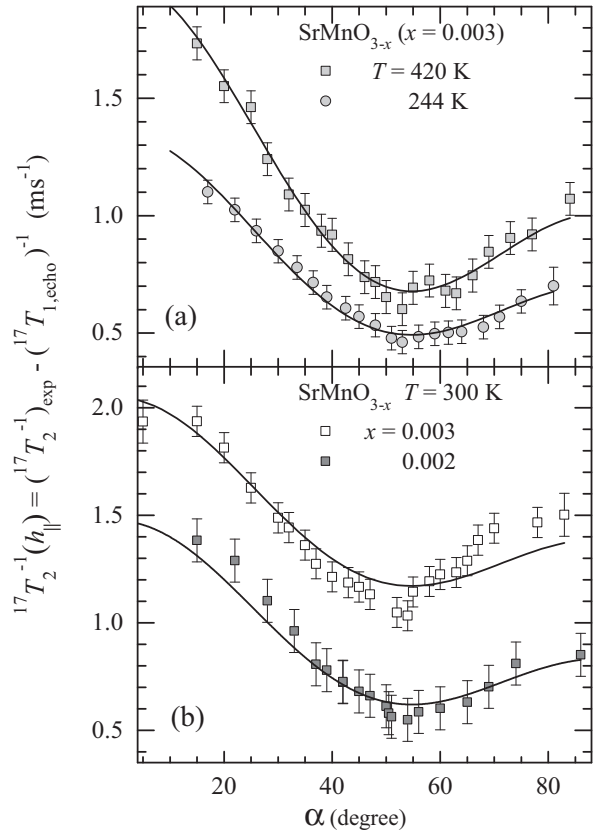

FIG. 7. ^{17}O spin-echo decay rate $^{17}T_2^{-1}(h_\parallel)$ vs α in (a) $SrMnO_{2.997}$ at $T = 244$ and 420 K and (b) in $SrMnO_{2.997}$ and $SrMnO_{2.998}$ at $T = 300$ K. The solid curves are the fits with the expression $a + b(1 - 3\cos^2\alpha)^2$.

The large experimental value of $^{17}T_2^{-1}(h_\parallel)$ is most likely due to an increase of $\langle(h_\parallel)^2\rangle$, created at oxygen by the neighboring $S(t_{2g})$ spins, $\boldsymbol{S}_1$, $\boldsymbol{S}_2$, which instant configuration is not only the ground state but also the excited triplet state ($\boldsymbol{S}_1 + \boldsymbol{S}_2 = 2\boldsymbol{S}$) with $h_{\parallel,\text{triplet}} \gg h_\parallel$. During the time τ_{singlet}, the ^{17}O resonance frequency, $\nu_{\text{singlet}} = \gamma h_{\parallel,\text{singlet}}$, it is about 0.1 MHz whereas during the time τ_{triplet}, $\nu_{\text{triplet}} = \gamma h_{\parallel,\text{triplet}}$ it is about 25 MHz [27]. The latter frequency value is far above our experimental NMR window in Fig. 1. The ratio $\tau_{\text{triplet}}/\tau_{\text{singlet}}$ is equal to $P_{\text{triplet}}/P_{\text{singlet}}$, the ratio of the probabilities to find the Mn neighbors in the triplet or singlet configurations. At $\tau_{\text{triplet}}/\tau_{\text{singlet}} \ll 1$ and for $^{17}T_{2,2p_\pi}^{-1}(h_\parallel) = (\gamma h_{\parallel,\text{triplet}} P_{\text{triplet}}/P_{\text{singlet}})^2 > 2\pi/\omega_{\text{ex}}$ [28,29] we get at room temperature the ratio $P_{\text{triplet}}/P_{\text{singlet}} = 0.08$. This value quantifies the proportion of FM and AF correlated $S(t_{2g})$ spin pairs which exist at room temperature in the PM phase of slightly electron doped as well as in *undoped* cubic $SrMnO_3$.

Let us now turn to ^{17}O and ^{17}Sr $T_{2,e_g}^{-1}(h_\parallel)$ rates defined by the time fluctuating component along $\boldsymbol{H}$, $h_{\text{hf},\parallel}(e_g)$, of the hyperfine fields $h_{\text{hf}}(e_g)$, where $h_{\text{hf},\parallel}(e_g)$ is proportional to $n_{e_g}(t)S_{z'}(t)$. This is in contrast with $^{17}T_{2,2p_\pi}^{-1}(h_\parallel)$ which expression, $^{17}T_{2,2p_\pi}^{-1}(h_\parallel) \propto \int_0^\infty d\tau\langle S_{z'}(\tau)S_{z'}(0)\rangle\cos(\omega\tau)$, does not depend on n_{e_g}. The rate $T_{2,e_g}^{-1}(h_\parallel)$ is proportional to

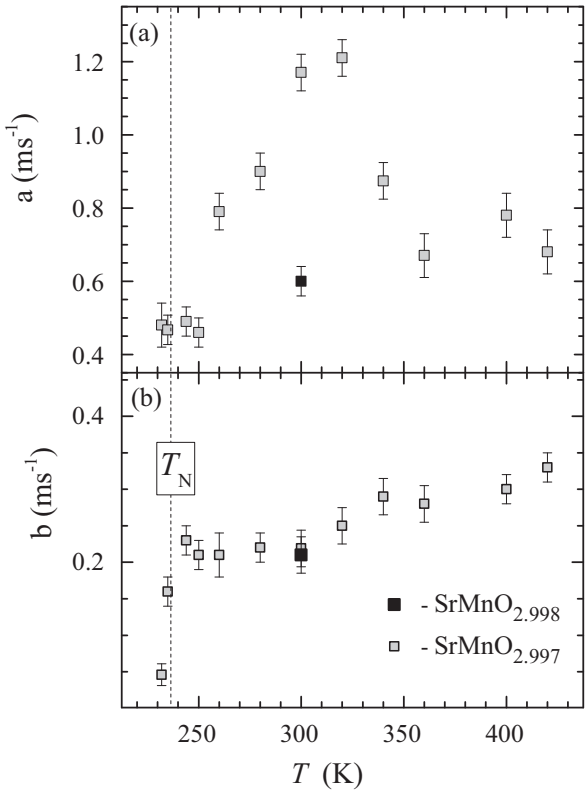

FIG. 8. Temperature dependence of (a) isotropic contribution $^{17}T_{2,e_g}^{-1}(h_\parallel) \equiv a$ and (b) anisotropic contribution $^{17}T_{2,2p_\pi}^{-1}(h_\parallel, \alpha) \equiv b(1 - 3\cos^2\alpha)^2$ to the rate $^{17}T_2(h_\parallel)^{-1}$.

the spectral intensity built at $\omega \ll \omega_{\mathrm{NMR}}$ by the product of the corelation functions $\langle n_{e_g}(t)n_{e_g}(0)\rangle$ and $\langle S_{z'}(t)S_{z'}(0)\rangle$. Indeed, the comparison of the two samples $SrMnO_{2.997}$ and $SrMnO_{2.998}$, shows that on one hand $T_{2,e_g}^{-1}(h_\parallel)$ is sensitive to the electron doping level since it decreases in the less doped $SrMnO_{2.998}$ and on the other hand, $^{17}T_{2,2p_\pi}^{-1}(h_\parallel)$ is not sensitive, as expected. The rate $T_{2,e_g}^{-1}(h_\parallel)$ shows an unusual behavior with a broad peak around 310 K in $SrMnO_{2.997}$ [Fig. 8(a)]. It is worth to note that at high frequencies $\omega = (1\text{–}4) \times 10^8$ s^{-1}, the thermal behavior of $\langle n_{e_g}(t)n_{e_g}(0)\rangle$ shows no anomaly as deduced from $^{17}T_1^{-1}(e_g)$ versus T data [Fig. 4(b)] in contrast to $T_{2,e_g}^{-1}(h_\parallel)$ which shows that at far lower frequencies $\langle n_{e_g}(t)n_{e_g}(0)\rangle$ leads to an abnormal growth of the fluctuating $^{17}h(e_g)$.

In $SrMnO_{2.997}$, the nonmonotonic variation of $^{17}T_{2,e_g}^{-1}(T)$ is caused by the slow-moving $(2x - n_{e_g})$ electrons which create pulselike fluctuations of the local field at the ^{17}O probe. Indeed, the slow diffusing motion of these electrons increases the efficiency of the DE mechanism, favoring FM correlated pairs of neighboring $S(t_{2g})$ spins in the Mn–^{17}O–Mn bond. This $^{17}T_{2,e_g}^{-1}(T)$ unusual behavior indicates the presence of fluctuations of some short-range magnetic order (SRMO) at low-frequency in the range $\omega_{\mathrm{srmo}} = 2\pi\, ^{17}T_2^{-1}(e_g)$, i.e., fluctuations slower than 10^3 s^{-1}. The SRMO includes the change of spin configurations from AF to FM order of the two Mn neighbors in an Mn–O–Mn bond during the time $^{17}T_{2,e_g}$.

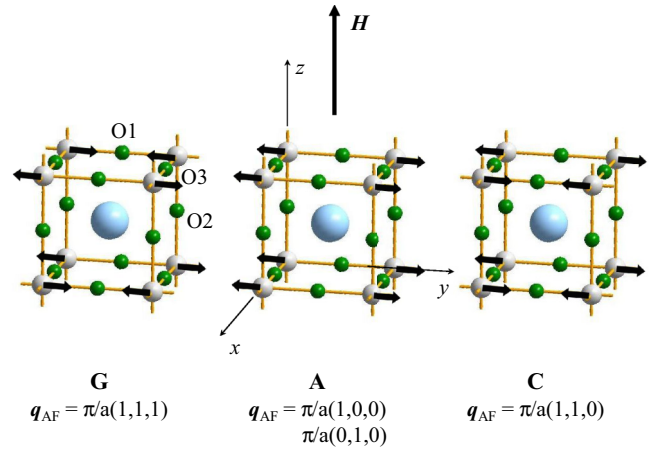

FIG. 9. AF spin configurations in the paramagnetic phase of cubic $SrMnO_{2.997}$ in the magnetic field $H = 117$ kOe.

In contrast to ^{17}O, the T dependence of $^{87}T_2^{-1}$ shows no anomaly (Fig. 5). Let us underline that each ^{17}Sr probes the spin configurations of eight nearest Mn neighbors. The absence of anomaly means that the sum $\Sigma^{8}{}_{i=1}h_i(e_g)$ is zero, even if during the time $^{87}T_2$ some pairs of $S(t_{2g})$ neighbors become FM correlated within the cubic unit cell. Thus, with the T_{2,e_g}^{-1} results, we deduce from ^{17}O that there is some short-range magnetic order at low-frequency whereas with ^{17}Sr, we deduce that FM order should be excluded within *the cubic unit cell*. So that the scrolling of different $S(t_{2g})$ environments experienced by both NMR probes O and Sr leads only to the following AF orders in the *cubic unit cell* (Fig. 9): AF–G $[\boldsymbol{q} = \pi/a(1, 1, 1)]$, AF–C $[\boldsymbol{q} = \pi/a(1, 1, 0)]$, and AF–A $[\boldsymbol{q} = \pi/a(0, 0, 1)]$ [3]. Thus in cubic $SrMnO_{3-x}$ the slow fluctuating short-range magnetic order is built from these three AF ordered unit cells. Being short range, the SRMO involves slow fluctuation of spin correlations of Mn neighbors in nanodomains built with a restricted number of unit cells; its proposed description is as follows. Pairs of neighboring AF coupled $S(t_{2g})$ spins fluctuate rapidly $(\uparrow\downarrow \leftrightarrow \downarrow\uparrow)$ with the time constant $\tau_c = 2\pi/\omega_{\mathrm{ex}}$, while the AF configurations of the eight $S(t_{2g})$ spins within the cubic unit cell is stable during a much longer time, $\tau_{c,\mathrm{srmo}} = 2\pi/\omega_{\mathrm{srmo}}$ corresponding to fluctuations slower than 10^3 s^{-1}. During this long time, the staggered moments of the spin configuration rotate perpendicularly to H minimizing the magnetic energy of these nanodomains, as $H > H_{\text{spin-flop}}$.[3]

The existence in the PM state of C and A-type AF configurated cubic cells which are of reduced dimensionality (Fig. 9) most likely explains the gaplike thermal behavior of the magnetic susceptibility.

[3]In the low-temperature phase, the value of $H_{\text{spin-flop}}$ is estimated as 20 kOe, with the expression $H_{\text{spin-flop}} = (H_a H_{\mathrm{ex}})^{0.5}$ using the magnetic field anisotropy $H_a = 200$ Oe and the exchange field $H_{\mathrm{ex}} = 1 \times 10^6$ Oe. In the PM phase this $H_{\text{spin-flop}}$ estimation is an upper limit.

IV. CONCLUSIONS

The manganese oxide $SrMnO_3$ with the $Pm\bar{3}m$ crystal structure is a rare example of cubic antiferromagnet. A lightly electron-doped $SrMnO_{2.997}$ polycrystalline sample has been studied in the PM phase with ^{17}O and ^{17}Sr NMR measurements.

The gaplike peculiar behavior of the bulk magnetic susceptibility $d\chi/dT \geqslant 0$, is due to the spin susceptibility χ_s of the localized spins $S(t_{2g})$ of the Mn ions, as deduced from ^{17}O and ^{17}Sr NMR shift data. Such T dependence of χ being typical of compounds with low dimensional AF configuration suggests that in the PM phase some short-range magnetic orders of the $S(t_{2g})$ spins with a lower-dimensional AF configuration should add to the main three dimensional AF–G type configuration. We have focused our study on the low-energy spin excitations in the PM phase by measuring the spin-lattice T_1^{-1} and the spin-echo decay T_2^{-1} rates of both probe nuclei in the PM phase. Thus the time-dependent part of the hyperfine fields $^{17}h(e_g)$, $^{87}h(e_g)$, and $^{17}h(2p_\pi)$ at low frequencies were investigated.

The thermal behavior of $^{17}T_1^{-1}(2p_\pi) \propto T$ indicates an almost T-independent value of the characteristic energy of the damped magnon excitations of the AF coupled $S(t_{2g})$ Mn spins, $\hbar\omega_{sf}$, at $q \ll \pi/a$. Moreover the deduced T-independent behavior of $\chi_s(q)/\omega_{sf}(q)$ ratio at $q \ll \pi/a$, indicates a high thermal stability of the fluctuating short-range magnetic order in the PM phase of $SrMnO_{2.997}$.

The echo-decay rate $^{17}T_2^{-1}$ probes the fluctuations of the neighboring $S(t_{2g})$ spins at $\omega \ll \omega_{nmr}$. The contribution $^{17}T_{2,e_g}^{-1}$ is proportional to the spectral intensity of the correlation function, $\langle n_{e_g}(t)n_{e_g}(0)\rangle$, where n_{e_g} is the number of fast-moving doped electrons per Mn with $n_{e_g} \leqslant 2x$. Consistently, our results show that $^{17}T_{2,e_g}^{-1}$ is sensitive to the electron doping level since it decreases from $SrMnO_{2.997}$ to the less doped sample $SrMnO_{2.998}$. As shown by our shifts data, n_{e_g} decreases down to T_N, so that a fraction $(2x - n_{e_g})$ of the doped e_g electrons slow down their Mn–Mn hopping providing local changes of the double-exchange interaction which favor FM correlated pairs of neighboring $S(t_{2g})$ spins in the $Mn - {}^{17}O - Mn$ bond. The rate $^{17}T_{2,e_g}^{-1}$ exhibits an unusual behavior with a broad peak around 310 K in $SrMnO_{2.997}$. This nonmonotonic variation which is caused by the slow-moving $(2x - n_{e_g})$ doped electrons indicates low-frequency ($\omega_{srmo} \leqslant 10^3\ s^{-1}$) fluctuations of the short-range magnetic order which may include the change of AF $\leftrightarrow$ FM spin alignment of neighboring magnetic ions.

For the ^{17}Sr nuclei, which probe the spin configuration of eight neighboring Mn in the cubic unit cell, there is no T_2^{-1} anomaly. With the $^{87}T_{2,e_g}^{-1}$ results, we deduce that FM order should be excluded within *the cubic unit cell*. Both NMR probes lead only to the following AF orders in the *cubic unit cells*: AF–G $[\boldsymbol{q} = \pi/a(1,1,1)]$, AF–G $[\boldsymbol{q} = \pi/a(1,1,0)]$, and AF–A $[\boldsymbol{q} = \pi/a(0,0,1)]$ so that the slow fluctuating short-range magnetic order is built from these three AF ordered unit cells shown in Fig. 9.

Finally, in contrast to the AF state where FM ordered nanoregions like small-size magnetic polarons are created by the doped electrons below 50 K, our study reveals that no FM ordered cubic unit cells may appear in the PM state so that more complicated AF short-range spin order exists above T_N in cubic $SrMnO_{3-x}$.

ACKNOWLEDGMENTS

The research was carried out within the state assignment of Ministry of Science and Higher Education of the Russian Federation (theme "Function" No. AAAA-A19-119012990095-0) and supported in part by the Russian Foundation of Basic Researches (project No. 18-32-00030). A.G. and S.V. are grateful to ESPCI for hospitality and support.

[1] T. Negas and R. Roth, J. Solid State Chem. **1**, 409 (1970).
[2] O. Chmaissem, B. Dabrowski, S. Kolesnik, J. Mais, D. E. Brown, R. Kruk, P. Prior, B. Pyles, and J. D. Jorgensen, Phys. Rev. B **64**, 134412 (2001).
[3] E. Wollan and W. Koehler, Phys. Rev. **100**, 545 (1955).
[4] A. Trokiner, S. Verkhovskii, Z. Volkova, A. Gerashenko, K. Mikhalev, A. Germov, A. Yakubovskii, A. Korolev, B. Dabrowski, and A. Tyutyunnik, Phys. Rev. B **93**, 174413 (2016).
[5] D. Teaney, M. Freiser, and R. Stevenson, Phys. Rev. Lett. **9**, 212 (1962).
[6] L. de Jongh and A. Miedema, Adv. Phys. **50**, 947 (2001).
[7] R. Coldea, R. A. Cowley, T. G. Perring, D. F. McMorrow, and B. Roessli, Phys. Rev. B **57**, 5281 (1998).
[8] A. A. Belik, Y. Matsushita, Y. Katsuya, M. Tanaka, T. Kolodiazhnyi, M. Isobe, and E. Takayama-Muromachi, Phys. Rev. B **84**, 094438 (2011).
[9] H. Sakai, S. Ishiwata, D. Okuyama, A. Nakao, H. Nakao, Y. Murakami, Y. Taguchi, and Y. Tokura, Phys. Rev. B **82**, 180409(R) (2010).
[10] C. Chiorescu, J. L. Cohn, and J. J. Neumeier, Phys. Rev. B **76**, 020404(R) (2007).
[11] H. Meskine, H. König, and S. Satpathy, Rhys. Rev. B **64**, 094433 (2001).
[12] J. van den Brink and D. Khomskii, Phys. Rev. Lett. **82**, 1016 (1999).
[13] A. M. Oleś and G. Khaliulin, Phys. Rev. B **84**, 214414 (2011).
[14] J.-S. Zhou and J. B. Goodenough, Phys. Rev. B **68**, 054403 (2003).
[15] P.-G. de Gennes, Phys. Rev. **118**, 141 (1960).
[16] A. Germov, A. Trokiner, Z. Volkova, K. Mikhalev, A. Gerashenko, S. Verkhovskii, A. Korolev, I. Leonidov, E. Konstantinova, and V. Kozhevnikov, Phys. Rev. B **96**, 104409 (2017).
[17] A. Narath, *Hyperfine Interactions* (Academic Press, New York, 1967).
[18] L. Vaugier, H. Jiang, and S. Biermann, Phys. Rev. B **86**, 165105 (2012).
[19] C. Zener, Phys. Rev. **82**, 403 (1951).

[20] E. Andrew and D. Tunstall, Proc. R. Soc. London **78**, 1 (1961).
[21] D. Freude and J. Haase, *Quadrupole eEffects in Solid-State Nuclear Magnetic Resonance* (Springer-Verlag, Berlin Heidelberg, 1993).
[22] C. Pennington, V. Stenger, C. Recchia, C. Hahm, K. Gorny, V. Nandor, D. Buffinger, S. Lee, and R. Ziebarth, Rhys. Rev. B **53**, R2967 (1996).
[23] C. Slichter, *Principles of Magnetic Resonance* (Springer-Verlag, Berlin, 1990), p. 640.
[24] R. Nathans, F. Menzinger, and S. Pickart, J. Appl. Phys. **39**, 1237 (1968).
[25] A. Narath, Phys. Rev. B **13**, 3724 (1976).
[26] R. Walstedt and S.-W. Cheong, Rhys. Rev. B **51**, 3163 (1995).
[27] A. Trokiner, S. Verkhovskii, A. Yakubovskii, A. Gerashenko, P. Monod, K. Kumagai, K. Mikhalev, A. Buzlukov, Z. Litvinova, O. Gorbenko, A. Kaul, and M. Kartavtzeva, Phys. Rev. B **79**, 214414 (2009).
[28] T. Kohmoto, T. Goto, S. Maegawa, N. Fujiwara, Y. Fukuda, M. Kunitomo, and M. Mekata, Phys. Rev. B **49**, 6028 (1994).
[29] S. Baek, F. Borsa, Y. Furukawa, Y. Hatanaka, S. Kawakami, K. Kumagai, B. Suh, and A. Cornia, Phys. Rev. B **71**, 214436 (2005).